



Published in final edited form as:

J Am Chem Soc. 2010 June 2; 132(21): 7514–7518. doi:10.1021/ja102482b.

Silver Nanoparticle-Catalyzed Diels-Alder Cycloadditions of 2'-Hydroxychalcones

Huan Cong, Clinton F. Becker, Sean J. Elliott, Mark W. Grinstaff, and John A. Porco Jr.*

Department of Chemistry and Center for Chemical Methodology and Library Development (CMLD-BU), Boston University, Boston, Massachusetts 02215

Abstract

Metal nanoparticles are currently being employed as catalysts for a number of classical chemical transformations. In contrast, identification of novel reactions of nanoparticles, especially towards the synthesis of complex natural products and derivatives, is highly underdeveloped and represents a burgeoning area in chemical synthesis. Herein, we report silica-supported silver nanoparticles as solid, recyclable catalysts for Diels-Alder cycloadditions of 2'-hydroxychalcones and dienes in high yield and turnover number. The use of silver nanoparticle catalysts is further demonstrated by the total synthesis of the cytotoxic natural product panduratin A employing a highly electron-rich dienophile and Lewis acid-sensitive diene.

Introduction

The 21st century is observing rapid progress in the nanosciences including preparation, characterization, and synthetic applications of metal nanoparticles.¹ Although nanoparticles are promising heterogeneous catalysts due to their high surface area and unique size-dependent properties,² they have not found substantial applications in complex natural product synthesis, with most examples thus far being limited to previously known transformations.³ This is in sharp contrast to homogeneous catalysts which are widely established and extensively used for a broad range of reaction types.⁴ Accordingly, the field of metal nanoparticle catalysis should offer opportunities for mining new chemical reactions,⁵ in particular, those which enable the synthesis of biologically important and synthetically challenging natural products and derivatives. Herein, we describe such an application involving the total synthesis of the bioactive cyclohexenyl chalcone natural product panduratin A which features silver nanoparticle (AgNP)-catalyzed Diels-Alder cycloadditions of 2'-hydroxychalcones and dienes.

Since its isolation in 1984,⁶ panduratin A (**1**) has shown promising anticancer, anti-HIV, and anti-inflammatory activities.⁷ This natural product belongs to the family of prenylflavonoid and related Diels-Alder natural products which are derived from highly oxygenated 2'-hydroxychalcone dienophiles.⁸ Behind the seemingly simple structure and straightforward retrosynthetic design of **1** (Scheme 1) are a number of synthetic challenges. The poorly reactive 2'-hydroxychalcone dienophile (*cf.* **2**) resists traditional Lewis acid-promoted conditions⁹ likely due to its electron-rich nature and the tendency of undesired cyclizations to form flavanones such as **3**. In addition, the requisite diene *trans*- β -ocimene (**4**) has been found to undergo olefin isomerization and polymerization under acidic conditions¹⁰ which complicates

porco@bu.edu.

Supporting Information Available: Experimental procedures and characterization data for AgNP catalyst and all new compounds. This material is available free of charge via the Internet at <http://pubs.acs.org>

chemical synthesis efforts. A recent report¹¹ outlined additional challenges in which thermal Diels-Alder cycloaddition (150 °C) of **4** and a 2'-hydroxychalcone dienophile afforded inseparable mixtures of **1** and its regioisomer isopanduratin A.¹²

Results and Discussion

Development of AgNP-catalyzed cycloadditions

Attempts to extend our reported methodology¹³ involving combined use of a Lewis acid (ZnI₂) and an electron donor (cobalt(I) complex or Bu₄NBH₄) to synthesize panduratin A were unsuccessful, underscoring the need for exploring alternative methodologies. Building upon our previous studies, we initiated an extensive screening of metal salts in combination with Bu₄NBH₄ for [4+2] cycloadditions of 2'-hydroxychalcones and dienes. Our studies revealed that using a mixture of 30 mol% AgBF₄ and 10 mol% Bu₄NBH₄, cycloaddition of 2'-hydroxychalcone **6** and 1-phenyl-3-methylbutadiene **7** afforded the desired cycloadduct **8** in 98% yield as a single regioisomer (Table 1, entry 1). A significant counterion effect of the silver salts was observed (entries 2–4), with AgPF₆, AgSbF₆, Ag₂CO₃, and Ag₂O showing poor reactivity. The success of the silver salt/borohydride catalyzed conditions was surprising as Ag(I) is a mild oxidant which is easily reduced to Ag(0) by borohydride.¹⁴ In contrast, silver (I) salts alone (entry 5), Bu₄NBH₄,¹³ or commercially available Ag powder¹⁵ displayed little or no reactivity in cycloadditions. In our reactions, a black, metallic silver precipitate was observed immediately after mixing the silver(I) salt and borohydride. Upon filtration, control experiments showed that the black precipitate had little reactivity, and that the clear supernatant accounted for catalytic activity (Table 1, entries 6, 7). A strong Tyndall effect of the supernatant¹⁵ suggested the presence of AgNP's¹⁶ which was further confirmed by transmission electron microscopy (TEM, Figure 1a), UV-Vis spectroscopy, and energy dispersive x-ray spectroscopy (EDS).¹⁵

Encouraged by these initial results, we next evaluated a heterogeneous and reusable catalyst preparation by fixation of the *in situ* generated, catalytically active AgNP's onto silica gel.¹⁷ In the optimized preparation, the AgNP-containing supernatant prepared from 3:1 AgBF₄/Bu₄NBH₄ in CH₂Cl₂ was stirred with chromatography-grade silica gel for 3 h in the air at 25 °C. Subsequent collection of the solid by filtration, followed by calcination at 220 °C for 12 h, afforded silica-supported AgNP's as a light brown powder (Figure 1b) containing 2.7 × 10² ppm of silver (approx. 70% Ag(0) and 30% Ag(I) as determined by X-ray photoelectron spectroscopy).¹⁵ The silica-supported AgNP's showed significantly higher catalytic activity than the corresponding *in situ* prepared AgNP's especially for cases involving highly electron-rich chalcones, likely due in part to removal of the capping ligands on the surface of AgNP during calcination.¹⁷

Cycloadditions catalyzed by the silica-supported AgNP generally favored the *endo* Diels-Alder cycloadducts with a single regioisomer observed for unsymmetrical dienes. Excellent yields and high turnover numbers (TON > 340, based on Ag loading) were obtained for cycloadditions between a number of 2'-hydroxychalcones and dienes under mild conditions using 0.25 mol% Ag loading (Table 2). Use of the supported AgNP catalyst at a loading as low as 0.01 mol% Ag afforded a nearly quantitative yield of cycloadduct **8** at a slightly higher temperature and prolonged reaction time (entry 2). Notably, reactions catalyzed by the silica-supported AgNP's were conducted in air without exclusion of oxygen or water. Moreover, the silica-supported AgNP catalyst could be stored on the bench-top for months and recycled without significant loss of activity (entries 3–6).

The silica-supported AgNP catalyst was next investigated for the synthesis of the cyclohexenyl chalcone natural product panduratin A. Initial silica-supported AgNP-catalyzed cycloadditions employing the unprotected 2',4',6'-trisubstituted chalcone **2**¹³ as dienophile were unsuccessful,

with the undesired flavanone **3** produced as a major byproduct likely due to the mild acidity of silica gel (*cf.* Scheme 1). We reasoned that a less electron-rich chalcone containing fewer free hydroxyl groups would be more optimal as a dienophile by minimizing side reactions. To our delight, cycloaddition of acetylated chalcone **15**¹³ and the labile diene **4** catalyzed by silica-supported AgNP's (0.5 mol% Ag loading) predominantly afforded the desired *endo* cycloadduct in excellent yield along with a small amount (approx. 5 %) of an *exo* stereoisomer corresponding to the natural product nicolaioidesin A.¹⁵ Neither isomerization nor polymerization of the labile diene was observed. Final deacetylation provided panduratin A in 87% yield (Scheme 2).

Mechanistic studies

Given the observed high activity and selectivity, we next conducted a series of experiments to probe the mechanism for AgNP-catalyzed Diels-Alder cycloadditions. Firstly, by filtering off the silica-supported AgNP catalyst after conducting the cycloaddition for 45 minutes, we observed no further conversion during the next five hours under the same conditions,¹⁵ indicating that the heterogeneous reaction involves minimal catalyst leaching¹⁸ and mechanisms entailing chain reactions are not likely operating. Secondly, kinetic data (Figure 2) of the silica-supported AgNP-catalyzed cycloadditions were obtained and are consistent with the Eley-Rideal kinetic model¹⁹ in which the 2'-hydroxychalcone adsorbs to the AgNP followed by reaction of the diene with the adsorbed substrate. Adsorption of the 2'-hydroxychalcone substrate to the AgNP surface was also evident by a significant red-shift²⁰ of the π - π^* band absorption of chalcone **6** from 318 nm to 370 nm in the absence and presence of *in situ*-generated AgNP's, respectively.¹⁵ Thirdly, we conducted electron paramagnetic resonance (EPR) measurements of a mixture of silica-supported AgNP catalyst, 2'-hydroxychalcone **15**, and CH₂Cl₂ in the presence of 5,5-dimethyl-1-pyrroline *N*-oxide (DMPO) as spin trap.²¹ We found that DMPO, the AgNP catalyst, and **15** were all necessary to observe EPR spectra (Scheme 3 and Figure 3) indicating the formation of DMPO adducts²² derived from radical species generated by the AgNP's and **15**.²³ The existence of radical species supports electron transfer processes between the AgNP and chalcone substrate, consistent with the known size-dependent redox potentials² and multiple oxidation states of AgNP's²⁴ as well as literature reports documenting electron transfer processes in metal nanoparticle-catalyzed reactions.^{3, 21, 25} We also observed partial formation of *p*-benzoquinone when *p*-hydroquinone was treated with the *in situ*-generated AgNP catalyst in the absence of an external oxidant,¹⁵ thus confirming the oxidative properties of the AgNP's.²⁶ Finally, we conducted cycloaddition of 2'-hydroxychalcone **6** and deuterium-labeled diene **D-7**²⁷ using the silica-supported AgNP's (Scheme 4). The exclusive *cis* relationship of the deuterium and the phenyl group derived from the diene in the cycloadducts supports a concerted cycloaddition mechanism. In comparison, cycloaddition of **6** and **D-7** using the ZnI₂/Bu₄NBH₄ conditions¹³ afforded cycloadducts with no preference for the position of deuterium, indicating a stepwise cycloaddition mechanism.¹⁵

Although we cannot completely rule out Lewis acid catalysis for [4+2] cycloadditions employing 2'-hydroxychalcones by coordinatively unsaturated sites on the AgNP surface,²⁸ based on our experimental results we propose the working mechanism shown in Scheme 5. Proton removal and single electron transfer (SET)²⁹ from the adsorbed chalcone **6** to the AgNP^{21a, 25} may generate the AgNP-stabilized phenoxy radical³⁰ intermediate **17a** which is in resonance with carbon-centered radical **17b**, a reactivity consistent with the antioxidant properties of natural 2'-hydroxychalcones.³¹ Concerted [4+2] cycloaddition³² between the activated dienophile **17a/b** and diene provides **18** which generates **19** *via* back electron transfer (BET) and protonation. A final desorption step turns over the catalytic cycle and releases cycloadduct **10** into solution. In the overall reaction, the AgNP's thus may serve as an "electron shuttle" catalyst^{25, 33} leading to highly selective activation of 2'-hydroxychalcones for

cycloadditions. In addition, no cycloadducts were observed when 2'-methoxychalcone was used as a dienophile employing the silica-supported AgNP catalyst¹⁵ indicating the requirement for the 2'-hydroxyl substituent of the chalcone substrate which is also consistent with the proposed mechanism.

Conclusion

We have developed a novel method for Diels-Alder cycloadditions of 2'-hydroxychalcones employing a silica-supported silver nanoparticle (AgNP) catalyst. The methodology has enabled highly efficient syntheses of cyclohexenyl chalcones which are found in a number of biologically active "Diels-Alder" natural products⁸ and the total synthesis of the natural product panduratin A using nanoparticle catalysis. To the best of our knowledge, this transformation represents the first example of a metal nanoparticle-catalyzed Diels-Alder cycloaddition. Initial mechanistic studies including EPR spin trapping experiments suggest that the cycloaddition involves a concerted process mediated by the AgNP's likely serving as an electron shuttle/redox catalyst. As communicated here, metal nanoparticles including AgNP's should find increasing applications for new chemical transformations, including those which enable the synthesis of complex natural products and derivatives. Further studies along these lines are currently in progress and will be reported in due course.

Supplementary Material

Refer to Web version on PubMed Central for supplementary material.

Acknowledgments

Financial support from the NIH (GM-073855), Merck, Wyeth, and AstraZeneca (graduate fellowship to H.C.) is gratefully acknowledged. This work made use of the MRSEC Shared Experimental Facilities at MIT, supported by the NSF (DMR-08-19762). We thank Professors J. Caradonna, L. Doerrer, B. Reinhard, S. Schaus (Boston University), and K. Moeller (Washington University, St. Louis) for helpful discussions. We also thank Drs. L. Yang, B. Liang, Y. Xiao, C. Prata; K. Milidakis, A. Griset, P. Tarves, B. Yan, S. Cantalupo (Boston University), L. Hu (Washington University, St. Louis), E. Shaw, and Dr. Y. Zhang (MIT) for instrumental assistance.

References

1. Schmid, G. Nanoparticles: From Theory to Application. Wiley-VCH; Weinheim: 2004.
2. Henglein A. Chem Rev 1989;89:1861–1873.
3. Astruc, D. Nanoparticles and Catalysis. Wiley-VCH; Weinheim: 2007.
4. Smith, MB.; March, J. March's Advanced Organic Chemistry: Reactions, Mechanisms, and Structure. 6. Wiley; Hoboken, NJ: 2007.
5. For select references, see: (a) Mitsudome T, Arita S, Mori H, Mizugaki T, Jitsukawa K, Kaneda K. Angew Chem Int Ed 2008;47:7938–7940. (b) Shimizu K, Sato R, Satsuma A. Angew Chem Int Ed 2009;48:3982–3986. (c) Murugadoss A, Goswami P, Paul A, Chattopadhyay A. J Mol Catal A 2009;304:153–158. (d) Witham CA, Huang W, Tsung C, Kuhn JN, Samorjai GA, Toste FD. Nature Chem 2009;2:36–41.
6. Tuntiwachwuttikul P, Pancharoen O, Reutrakul V, Byrne LT. Aust J Chem 1984;37:449–453.
7. For select references on biological activities of panduratin A, see: (a) Kiat TS, Phippen R, Yusof R, Ibrahim H, Khalid N, Rahman NA. Bioorg Med Chem Lett 2006;16:3337–3340. [PubMed: 16621533] (b) Yun JM, Kweon MH, Kwon H, Hwang JK, Mukhtar H. Carcinogenesis 2006;27:1454–1464. [PubMed: 16497706] (c) Cheenpracha S, Karalai C, Ponglimanont C, Subhadhirasakul S, Tewtrakul S. Bioorg Med Chem 2006;14:1710–1714. [PubMed: 16263298] (d) Kirana C, Jones GP, Record IR, McIntosh GH. J Nat Med 2007;61:131–137. (e) Shim JS, Kwon YY, Han YS, Hwang JK. Planta Med 2008;74:1446–1450. [PubMed: 18683126] (f) Yoshikawa M, Morikawa T, Funakoshi K, Ochi M, Pongpiriyadacha Y, Matsuda H. Heterocycles 2008;75:1639–1650. (g) Rukayadi Y, Lee K, Han S, Yong D, Hwang JK. Antimicrob Agents Chemother 2009;53:4529–4532. [PubMed: 19651906]

8. (a) Nomura T. *Pure Appl Chem* 1999;71:1115–1118. (b) Nomura T. *Yakugaku Zasshi* 2001;121:535–556. [PubMed: 11494599]
9. Corbett JL, Weavers RT. *Synth Commun* 2008;38:489–498.
10. Majetich G, Zhang Y. *J Am Chem Soc* 1994;116:4979–4980.
11. Chee CF, Abdullah I, Buckle MJC, Rahman NA. *Tetrahedron Lett* 2010;51:495–498.
12. For select references on isolation and biological activities of isopanduratin A, see: (a) Pandji C, Grimm C, Wray V, Witte L, Proksch P. *Phytochemistry* 1993;34:415–419. (b) Hwang JK, Chung JY, Baek NI, Park JH. *Int J Antimicrob Agents* 2004;23:377–381. [PubMed: 15081087] (c) Win NN, Awale S, Esumi H, Tezuka Y, Kadota S. *J Nat Prod* 2007;70:1582–1587. [PubMed: 17896818]
13. Cong H, Ledbetter D, Rowe GT, Caradonna JP, Porco JA Jr. *J Am Soc Chem* 2008;130:9214–9215.
14. Ganem B, Osby JO. *Chem Rev* 1986;86:763–780.
15. See Supporting Information for complete experimental details.
16. The Tyndall effect refers to the capacity of disperse or colloidal systems when illuminated unilaterally to scatter light in all directions, see: (a) Kraemer EO, Dexter ST. *J Phys Chem* 1927;31:764–782. (b) Roucoux A, Schulz J, Patin H. *Chem Rev* 2002;102:3757–3778. [PubMed: 12371901]
17. Zheng N, Stucky GD. *J Am Chem Soc* 2006;128:14278–14280. [PubMed: 17076500]
18. Pachon AD, Rothenberg G. *Appl Organometal Chem* 2008;22:288–299.
19. The Eley-Rideal mechanism refers to bimolecular, heterogeneous reactions in which only one reactant adsorbs to the catalyst surface, followed by a second reactant which reacts with the adsorbed reactant directly, see: Masel, RI. *Principles of Adsorption and Reaction on Solid Surfaces*. Wiley; Hoboken, NJ: 1996.
20. (a) Lim IS, Goroleski F, Mott D, Kariuki N, Ip W, Luo J, Zhong CJ. *J Phys Chem B* 2006;110:6673–6682. [PubMed: 16570972] (b) Nawrocka A, Krawczyk S. *J Phys Chem A* 2008;112:10233–10241.
21. For select examples outlining use of EPR spin trapping experiments to probe mechanisms of nanoparticle-catalyzed reactions, see: (a) Grirrane A, Corma A, García H. *Science* 2008;322:1661–1664. [PubMed: 19074342] (b) Conte M, Miyamura H, Kobayashi S, Chechik V. *J Am Chem Soc* 2009;131:7189–7196. [PubMed: 19405535]
22. (a) Buettner GR. *Free Radical Biol Med* 1987;3:259–303. [PubMed: 2826304] (b) Cholvad V, Szaboova K, Stasko A, Nuyken O, Voit B. *Magn Reson Chem* 1991;29:402–404. (c) Guo Q, Qian SY, Mason RP. *J Am Soc Mass Spectrom* 2003;14:862–871. [PubMed: 12892910] (d) Pinteala M, Schlick S. *Polym Degrad Stab* 2009;94:1779–1787.
23. The experimental EPR spectrum was fitted by superposition of signals from two DMPO adducts and a DMPO degradation radical. The hyperfine coupling constants and the ratio of the ^{14}N and H_β splittings of the simulated spectra are consistent with the DMPO adducts originating from carbon-centered radicals. The observation of more than one DMPO adduct could be attributed to multiple resonance structures of the original radicals derived from **15**.
24. Branham MR, Douglas AD, Mills AJ, Tracy JB, White PS, Murray RW. *Langmuir* 2006;22:11376–11383. [PubMed: 17154628]
25. For a recent example of an AgNP-catalyzed reaction involving electron transfer, see: Sudrik SG, Chaki NK, Chavan VB, Chavan SP, Chavan SP, Sonawane HR, Vijayamohan K. *Chem Eur J* 2006;12:859–864.
26. For select examples of AgNP-catalyzed oxidations, see: ref ^{5(a)–(c)}, and (a) Xu R, Wang D, Zhang J, Li Y. *Chem Asian J* 2006;1:888–893. [PubMed: 17441132] (b) Debecker DP, Faure C, Meyre ME, Derre A, Gaigneaux EM. *Small* 2008;4:1806–1812. [PubMed: 18844300] (c) Mitsudome T, Mikami Y, Funai H, Mizugaki T, Jitsukawa K, Kaneda K. *Angew Chem Int Ed* 2008;47:138–141.
27. Herndon JW, Hill DK, McMullen L. *Tetrahedron Lett* 1995;36:5687–5690.
28. Shimizu K, Sugino K, Sawabe K, Satsuma A. *Chem Eur J* 2009;15:2341–2351.
29. For select reviews on SET-initiated reactions, see: (a) Floreancig PE. *Synlett* 2007:191–203. (b) Moeller KD. *Synlett* 2009:1208–1218. (c) Li CJ. *Acc Chem Res* 2009;42:335–344. [PubMed: 19220064]
30. Zhang Z, Berg A, Levanon H, Fessenden RW, Meisel D. *J Am Chem Soc* 2003;125:7959–7963. [PubMed: 12823017]

31. Kozłowski D, Trouillas P, Calliste C, Marsal P, Lazzaroni R, Duroux JL. *J Phys Chem A* 2007;111:1138–1145. [PubMed: 17253666]
32. For pioneering studies on electron transfer-initiated, radical cation-mediated Diels-Alder cycloadditions, see: Bauld, NL. *Tetrahedron*. Vol. 45. 1989. p. 5307-5363.. Attempts to apply Bauld's aminium ion catalyst [*tris*(4-bromophenyl)ammoniumyl hexachloroantimonate] to Diels-Alder cycloadditions of 2'-hydroxychalcones and dienes were unsuccessful, thus illustrating the unique catalytic properties of AgNP's.
33. Mallick K, Witcomb M, Scurrall M. *Mater Chem Phys* 2006;97:283–287.

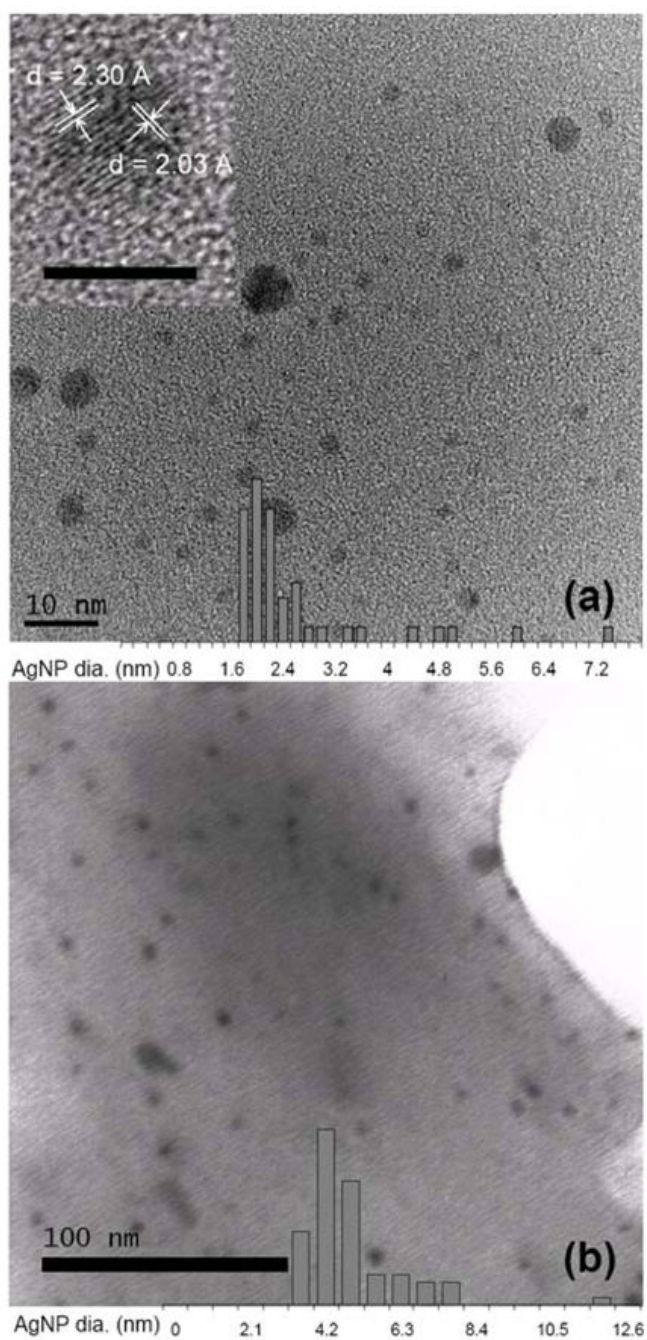


Figure 1. TEM images with particle size distribution histograms. (a) AgNP catalyst generated *in situ* from 3:1 AgBF₄/Bu₄NBH₄ showing an average particle size of 2.5 nm. Inset: high resolution TEM of a single particle with lattice d-spacing of 2.30 Å and 2.03 Å, matching the (111) and (200) plane of Ag with a face-centered cubic (fcc) structure, respectively. Inset scale bar: 5 nm. (b) Silica-supported AgNP catalyst showing an average particle size of 4.9 nm.

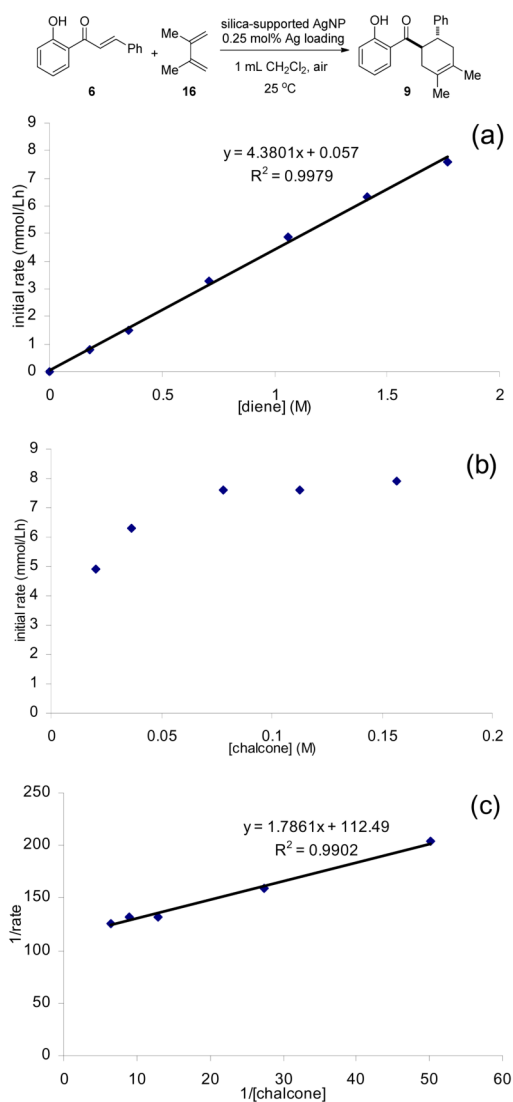


Figure 2. Kinetic plots of silica-supported AgNP-catalyzed Diels-Alder cycloadditions. (a) Initial rate as a function of diene concentration, indicating first-order kinetics in diene concentration. (b) Initial rate as a function of chalcone concentration. (c) Lineweaver-Burk plot confirming saturation kinetics in chalcone concentration.

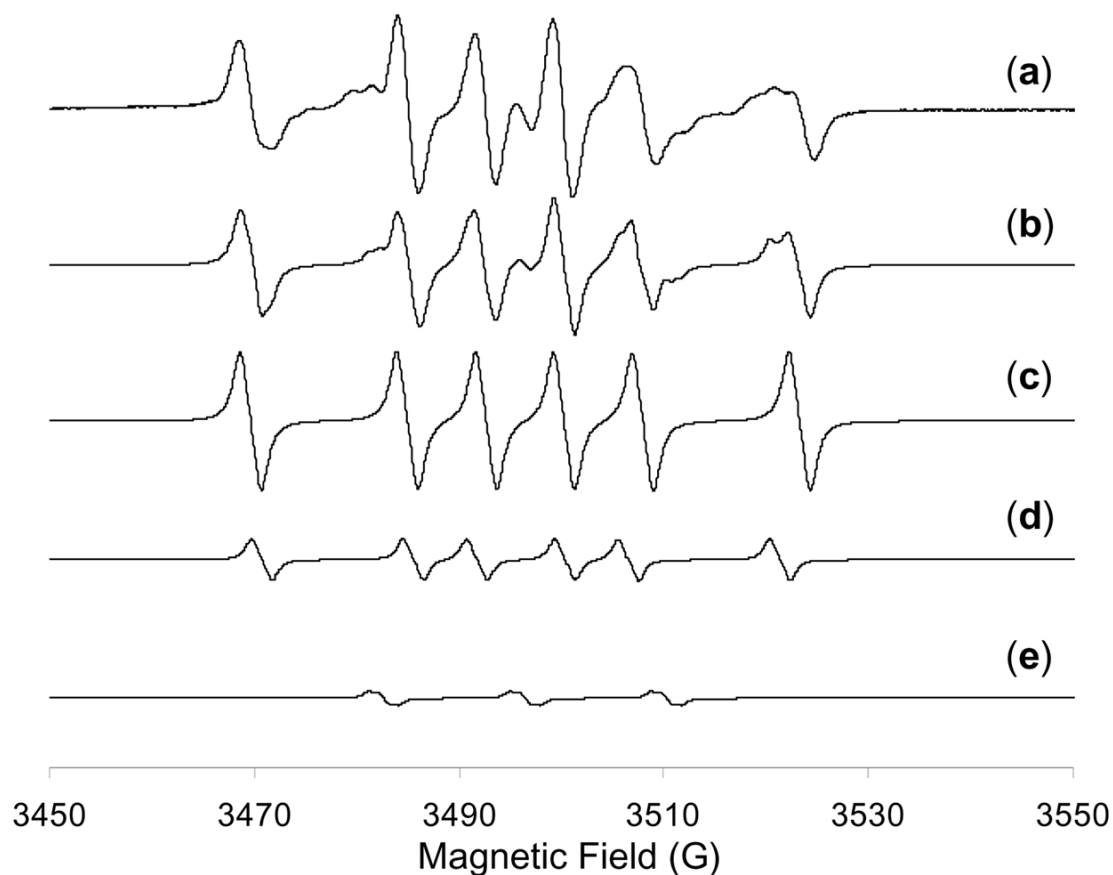
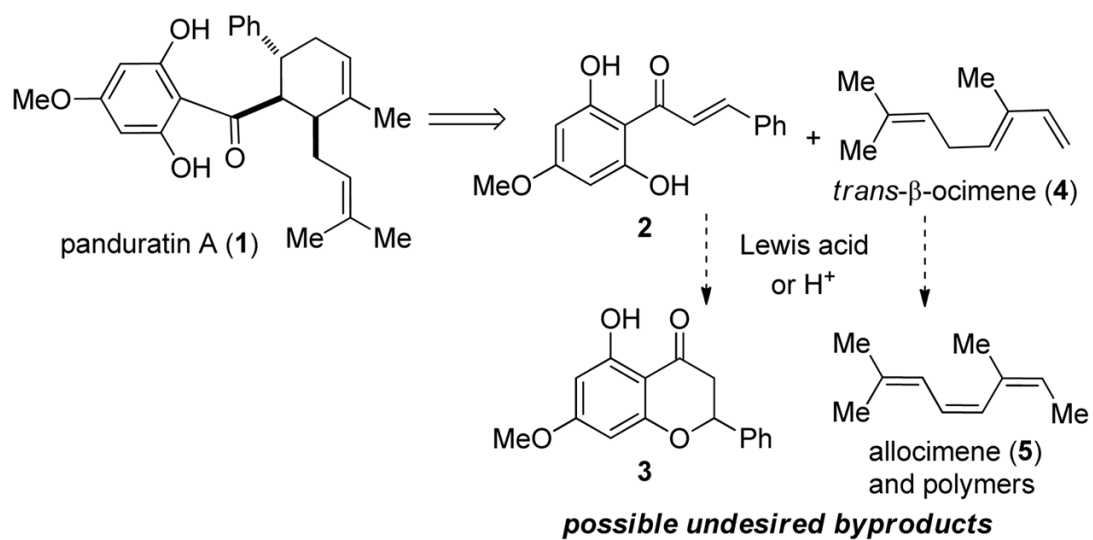
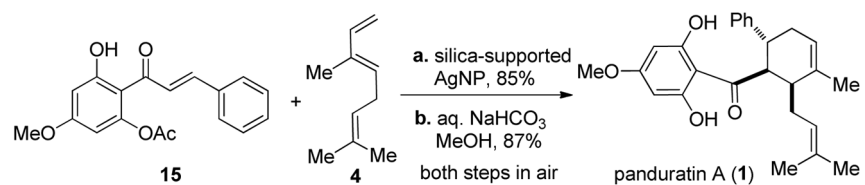


Figure 3.

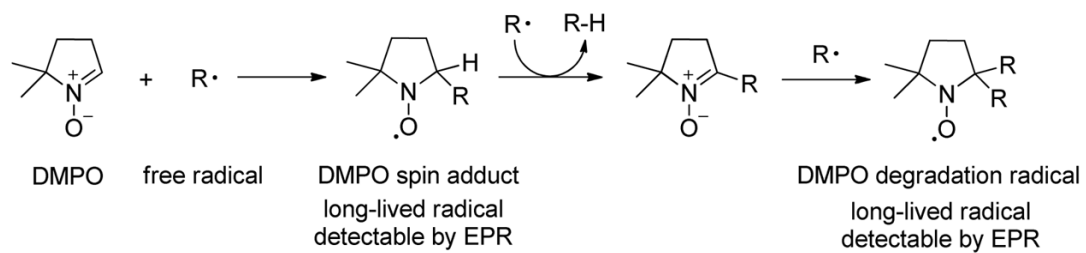
EPR spectra and computer simulation of spin trapping. (a) Experimental EPR spectrum obtained from a mixture of silica-supported AgNP catalyst (150 mg), 2'-hydroxy-4'-methoxy-6'-acetoxychalcone **10** (11.2 mg, 0.05 mmol), and DMPO (20 μ L, 0.18 mmol) in CH_2Cl_2 (0.5 mL) at 25 $^\circ\text{C}$. (b) Overall composite simulation. (c) Simulated spectrum of a DMPO/carbon-centered radical adduct. Composition: 71%. Linewidth: 0.85 G. Coupling constants: $a_{\text{N}} = 15.3$ G, $a_{\text{H}\beta} = 23.0$ G. (d) Simulated spectrum of a DMPO/carbon-centered radical adduct. Composition: 22%. Linewidth: 0.70 G. Coupling constants: $a_{\text{N}} = 14.8$ G, $a_{\text{H}\beta} = 21.0$ G. (e) Simulated spectrum of a DMPO degradation radical. Composition: 7%. Linewidth: 0.60 G. Coupling constants: $a_{\text{N}} = 13.8$ G, $a_{\text{H}\gamma} = 1.0$ G.

**Scheme 1.**

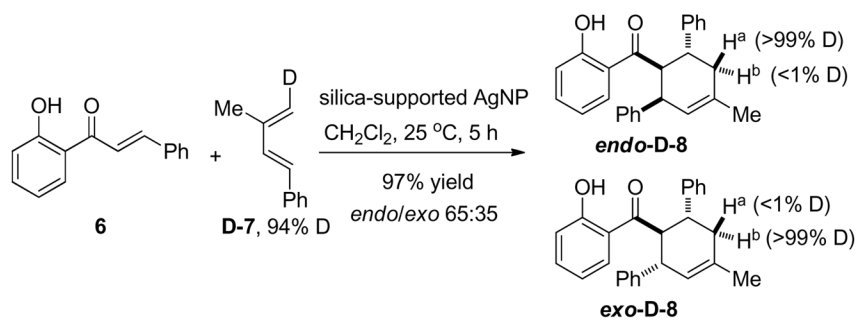
Retrosynthetic analysis for panduratin A and synthetic challenges.

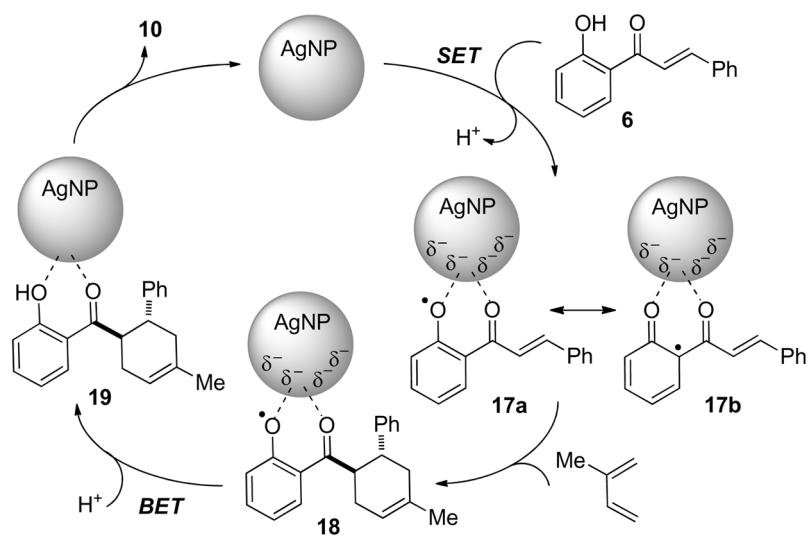
**Scheme 2.**Synthesis of (\pm)-panduratin A.^a

^aReagents and conditions: (a) Silica-supported AgNP (0.5 mol% Ag loading), CH₂Cl₂, 50 °C, 48 h, 85%. Major isomer shown; (b) aq. NaHCO₃, MeOH, 40 °C, 6 h, 87% (98% based on recovered starting material).

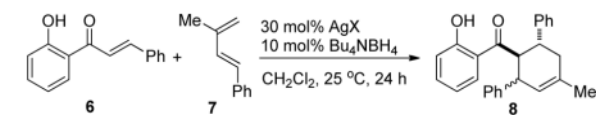
**Scheme 3.**

Chemical transformations leading to the formation of DMPO spin adducts and a DMPO degradation radical.

**Scheme 4.**Use of a deuterium-labeled diene.^a^aIsolated cycloadducts contained a trace amount of **8** (less than 10%) due to the presence of approximately 6% non-deuterium-labeled diene in starting material **D-7**.



Scheme 5.
Generalized mechanism for AgNP-catalyzed cycloadditions.

Table 1Discovery of AgNP-catalyzed Diels-Alder cycloadditions.^a

entry	AgX	conversion (%)	<i>endo/exo</i>
1	AgBF ₄	>99(98)	76:24
2	AgOTf	48	71:29
3	AgClO ₄	68	60:40
4	AgOAc	91	53:47
5 ^b	AgBF ₄	21	67:33
6 ^c	AgBF ₄	14	-
7 ^d	AgBF ₄	>99	78:22

^aConversions and *endo/exo* ratios are based on ¹H NMR integration. Isolated yield is shown in parentheses. Single regioisomer was observed.

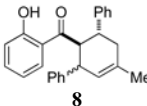
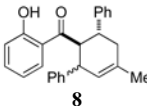
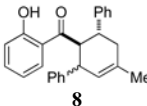
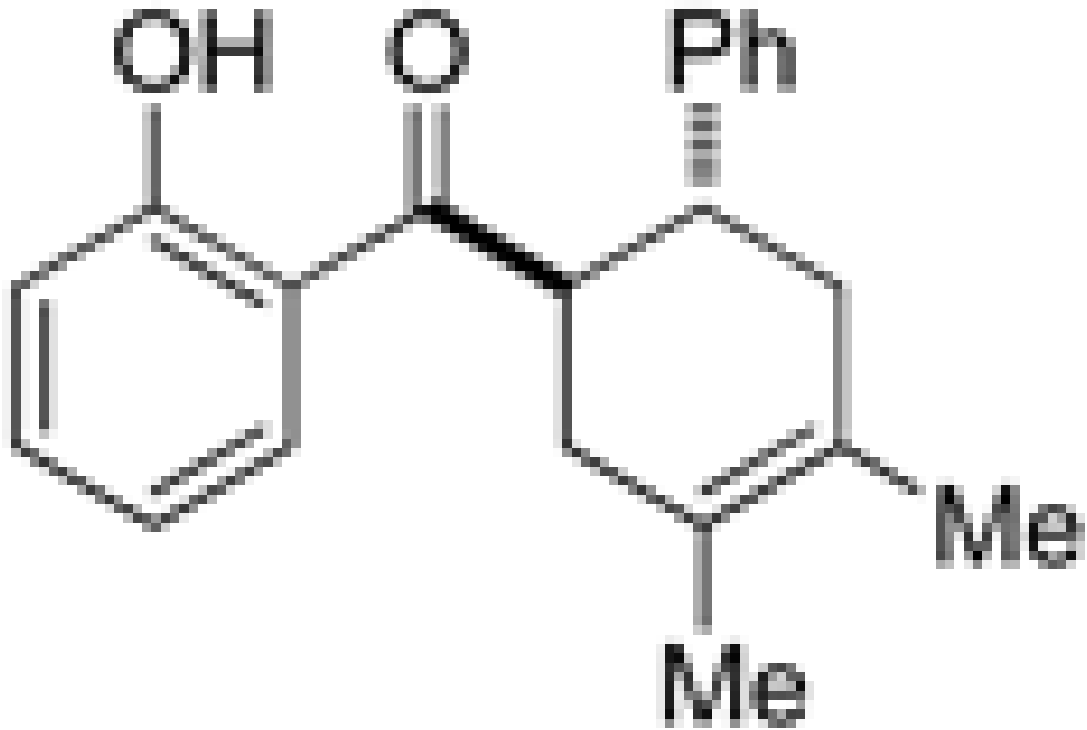
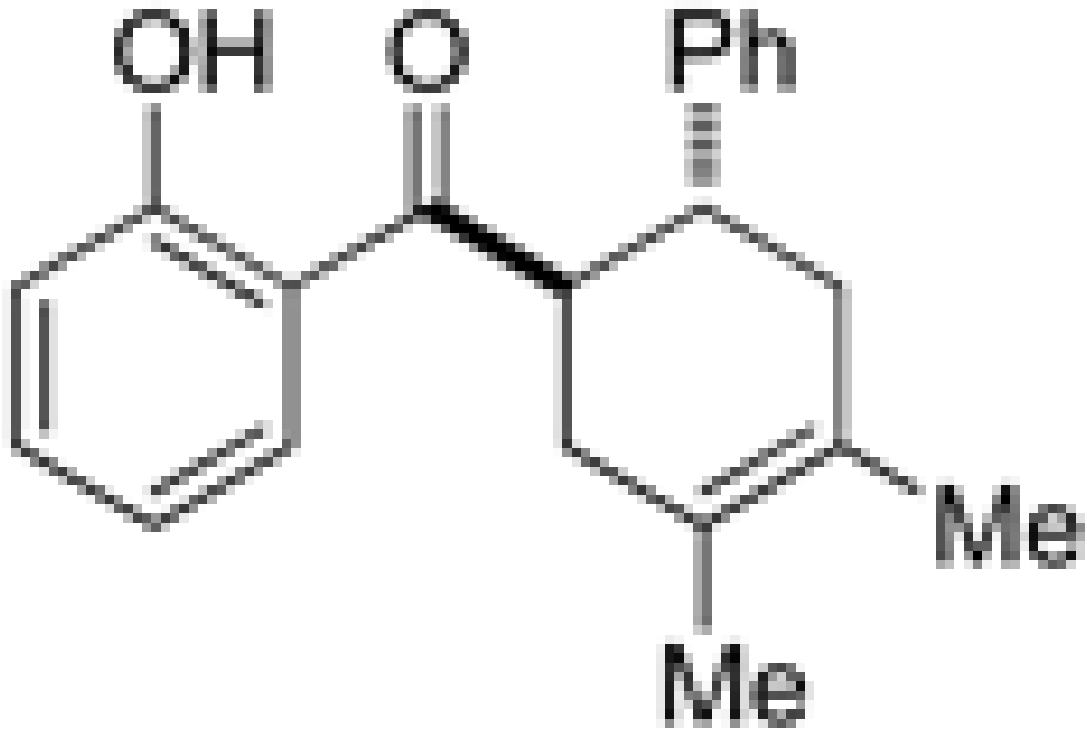
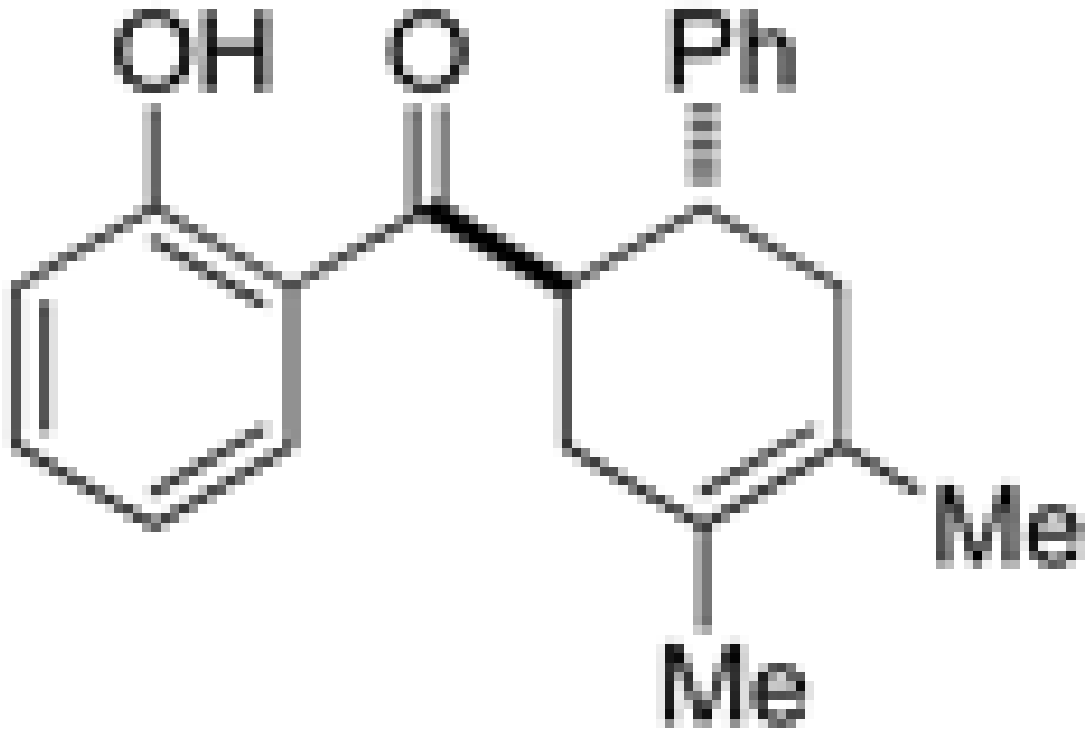
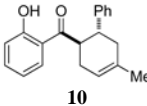
^b30 mol% AgBF₄ only.

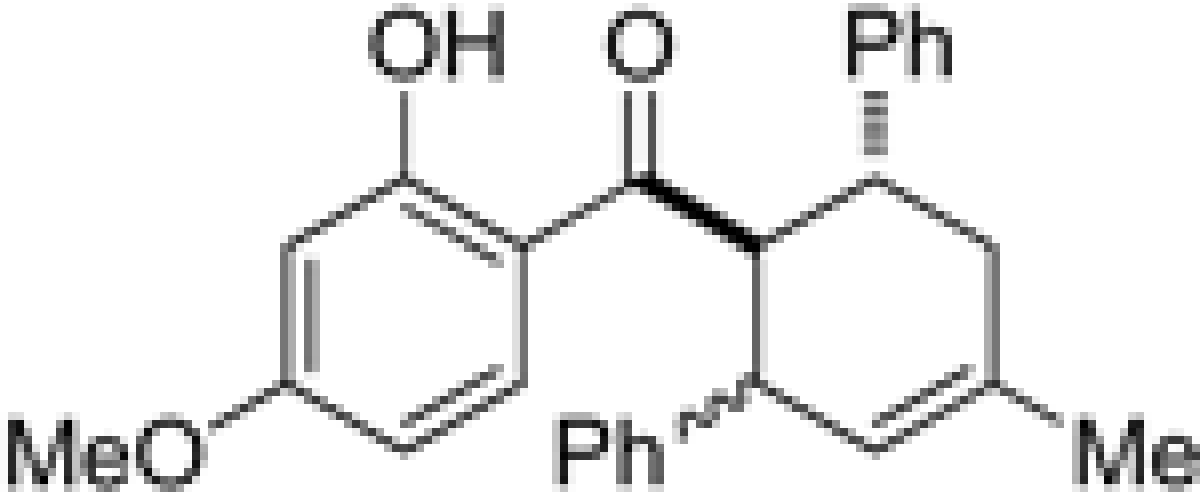
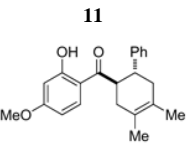
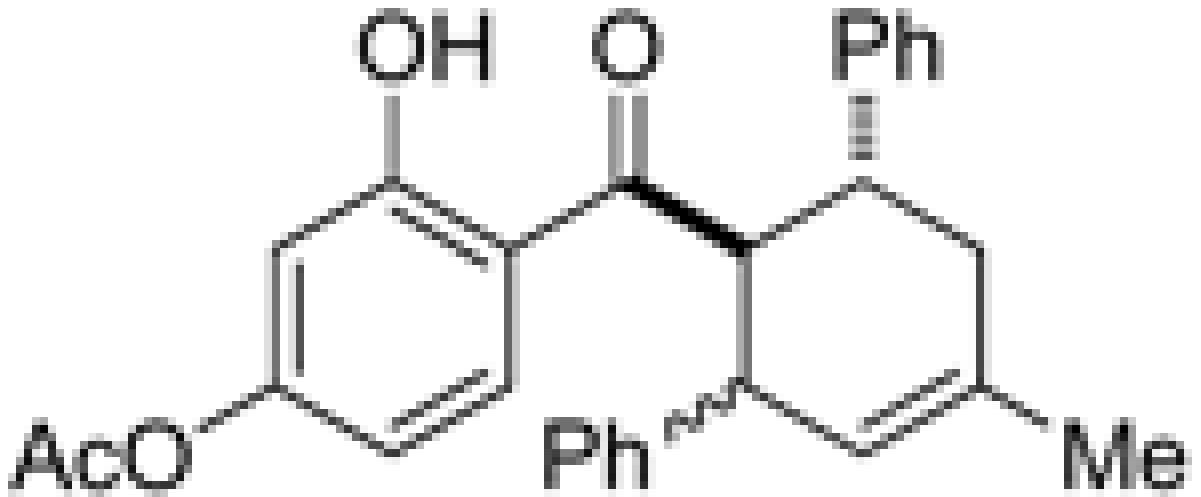
^cBlack precipitate only.

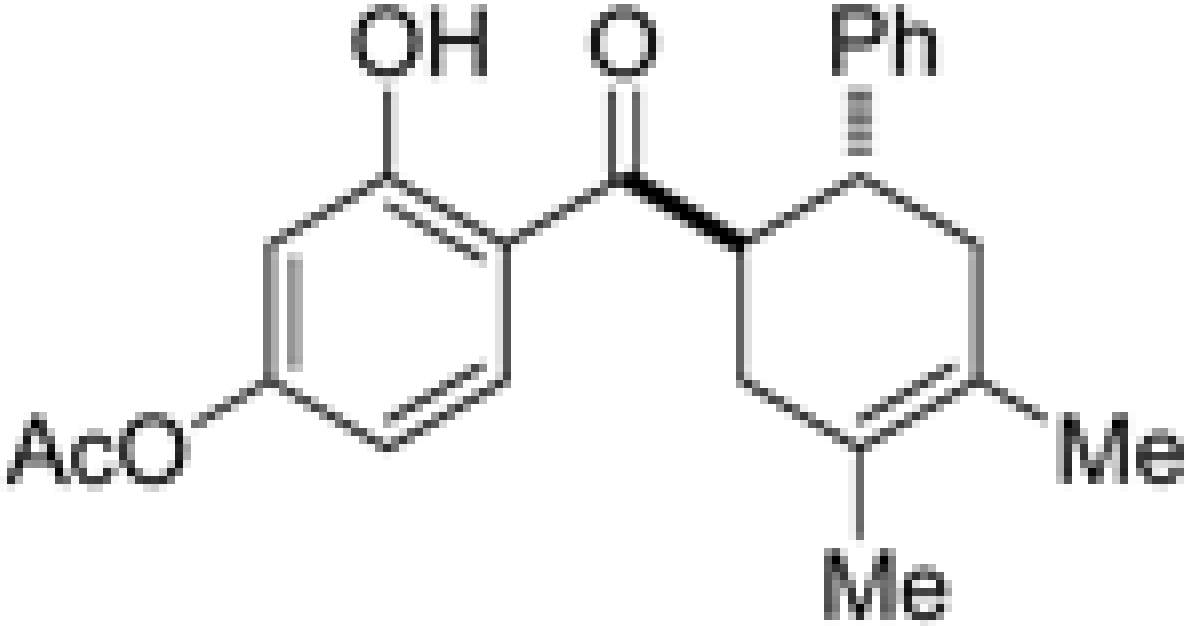
^dClear supernatant only.

Table 2

Silica-supported AgNP-catalyzed Diels-Alder cycloadditions.

entry	product	condition
1		0.25 mol AgNP, 40 °C, 5 h
2		0.01 mol AgNP, 40 °C, 36 h
3		0.25 mol AgNP, 40 °C, 5 h
4		Reused cat. 1st, 40 °C, 5 h
5		Reused cat. 2nd, 40 °C, 5 h
6		Reused cat. 3rd, 40 °C, 5 h
7		0.25 mol AgNP, 40 °C, 10 h

entry	product	condition
8	 <p>11</p>	0.25 mo AgNP, 4 C, 18 h
9	 <p>12</p>	0.25 mo AgNP, 4 C, 36 h
10	 <p>13</p>	0.25 mo AgNP, 4 C, 6 h

entry	product	condition
11		0.25 mol% AgNP, 4 h, 60 °C, 10 h

14

^aReactions conducted with 0.1 mmol 2'-hydroxychalcone substrate in 1 mL of CH₂Cl₂ in air using 100 mg of silica-supported AgNP catalyst (contains 27 μg Ag, 0.25 mol% Ag loading).

^bIsolated yields are shown with *endo/exo* ratio in parentheses. Single regioisomers observed for unsymmetrical dienes.

^cUsing 4.5 mg of silica-supported AgNP catalyst (contains 1.2 μg Ag, 0.01 mol% Ag loading).